Desalination and Water Treatment
www.deswater.com
doi: 10.5004/dwt.2022.28660

267 (2022) 215–230
August

Persulfate-enhanced lanthanum iron oxide-mediated photocatalysis can effectively degrade an aqueous industrial dye and mineralize water and wastewater

Olga Koba-Ucun[a], Idil Arslan-Alaton[a,*], Isabella Natali Sora[b], Miray Bekbölet[c]

[a]*Department of Environmental Engineering, School of Civil Engineering, Ayazaga Campus, 34465 Maslak, Istanbul, Turkey, Tel. +90 212 285 37 86; email: arslanid@itu.edu.tr (I. Arslan-Alaton)*
[b]*INSTM and Department of Engineering and Applied Sciences, University of Bergamo, Dalmine, Italy*
[c]*Institute of Environmental Sciences, Bogazici University, 34342 Bebek, Istanbul, Turkey*

Received 27 April 2022; Accepted 3 July 2022

ABSTRACT

A novel, home-made lanthanum iron oxide (LF; 0.125–1.00 g/L) was used to treat an industrial model pollutant (Reactive Black 5 dye-RB5; C_o = 20 mg/L) under UV-A irradiation (1.3 W/L). Aqueous, hydrolyzed RB5 solution that was prepared to mimic reactive dyehouse effluent could be successfully degraded by LF-mediated photocatalytic treatment and the degradation rate was remarkably enhanced in the presence of persulfate (PS; 0.6–1.2 mM). LF-mediated heterogeneous photocatalysis was only effective at pH ≤ 4. The dissolved organic carbon (DOC) content of the aqueous RB5 solution (DOC_o = 5.15 mg/L) could also be substantially removed by LF/UV-A (LF = 0.5 g/L; 52%–54% DOC removal after 150–180 min) and PS-enhanced LF/UV-A (LF = 0.5 g/L; 60%–66% DOC removal after 120 min). Reuse of the same LF photocatalyst for complete color and partial DOC removals was confirmed for the selected LF/UV-A/pH3 and LF/PS/UV-A/pH3 treatment conditions in four treatment cycles. LF/UV-A/pH3 and LF/PS/UV-A/pH3 were also applied to real water and wastewater samples; tap water (DOC_o = 1.98 mg/L) and two secondary treated sewage (DOC_o = 5.39 and 16.83 mg/L) samples. A decrease in DOC removals to 25% (tap water), 22% (secondary treated, low-DOC sewage sample) and 5% (secondary treated, high-DOC sewage sample) was observed for the real water and wastewater samples.

Keywords: Reactive Black 5 dye; Color and organic carbon removals; Lanthanum iron oxide-mediated photocatalysis; Persulfate; Photocatalyst reuse; Real water and wastewater treatment

1. Introduction

Perovskite-type oxides (general formula: "ABO_3") consist of a three-dimensional network of "BO_6" octahedron surrounding "A" metal cations. Generally, A-site cations are large size cations (Bi, La, Sr, etc.); B-site cations are transition metal cations (Fe, Cu, Mn, Cr, etc.) [1]. Perovskite oxides have various applications as gas sensors [2], solid oxide fuel cells [3], multiferroic materials [4] and photocatalysts for water/wastewater treatment [5–7]. They have received great interest because of their attractive physicochemical properties including photocatalytic activity even under near-UV/visible light radiation [1,8]. Decomposition of aqueous hydrogen peroxide (H_2O_2) over perovskite oxides under UV/visible irradiation has already been shown to enhance the oxidation of organic pollutants acting as semiconductor-type photocatalysts and/or heterogeneous Fenton-like treatment systems [8–10]. They became alternative materials for the degradation of environmental contaminants by initiating electron transfer reactions due to their good

* Corresponding author.

catalytic activity with minor leaching of transition metals, high stability and relatively simple synthesis procedures [1,2–8]. Previous work also indicated that the semiconductor $LaFeO_3$ (lanthanum iron oxide; called LF herein) has a great potential to degrade organic pollutants found in water and wastewater as good alternatives to more traditional heterogeneous semiconductor-type photocatalysts such as titanium dioxide, zinc oxide, or cadmium sulfide owing to their high electron mobility and relatively narrow band gap [6–8,10,11].

Industrial wastewater treatment remains a serious problem in developing countries. Among industrial effluents, textile industry wastewater is known for its refractory nature [12–14] mainly because of the use of various dyes and auxiliary chemicals of high chemical complexity [15]. Among the textile industry dyes, fiber reactive dyes which are used for the dyeing of natural (cotton) as well as synthetic (cellulose acetate) fibers, deserve special attention since they cannot be used after the dyeing process and end up in the spent reactive dyebath effluent in their hydrolyzed, unfixed form [15,16]. In fact, commercial dyes including fiber reactive dyes are specially designed to resist biological degradation, photolytic/photochemical as well as thermal decomposition rendering difficult-to-treat chemicals. Hence, the concentration of spent (hydrolyzed, unfixed) reactive dyes can easily reach mg/L levels in receiving natural water bodies [14,15]. It is expected that textile dyes have serious long-term effects on aquatic and terrestrial ecosystems due to their xenobiotic nature [15,17,18].

Several advanced treatment methods such as adsorption, membrane operations, chemical oxidation processes as well as advanced oxidation processes (AOPs; such as sonolysis, Fenton, photo-Fenton, semiconductor-mediated heterogeneous photocatalysis, catalytic ozonation, perozonation, etc.) have already been examined for color removal recently with good results [17–19]. However, in some developing and industrialized countries the color parameter has not well-defined specific discharge limits since it is economically and technically hard to achieve effective color removal [20,21]. Hence, although several chemical, photochemical and photocatalytic advanced treatment methods have already been published in the past, color removal from dyehouse effluent remains an expensive, problematic and difficult task.

AOPs are generally based on the formation of free radical species (active oxidants) that are used to oxidize a variety of organic pollutants including textile dyes. More recently, sulfate radical ($SO_4^{\bullet-}$)-based AOPs have attracted great attention as alternative treatment processes for micropollutants found in water/wastewater to hydroxyl radical ($HO^{\bullet}$)-based AOPs. The sulfate radical ($SO_4^{\bullet-}$) has a standard oxidation potential of E^0 = 2.5–3.1 eV vs. SHE [22–25]. Compared to $HO^{\bullet}$ (E^0 = 1.8–2.7 eV vs. SHE), the oxidation potential is quite similar. However, the main difference between these two free radicals comes from the half-life time ($t_{1/2}$ = 30–40 μs for $SO_4^{\bullet-}$ and only 20 ns for $HO^{\bullet}$), that renders $SO_4^{\bullet-}$ much more selective than the $HO^{\bullet}$ in the degradation of organic micropollutants [25–27]. $SO_4^{\bullet-}$ can be generated via several activation methods of for example the peroxide persulfate (PS) with zero-valent metals, transition metal ions, metal oxides, heat, UV-C irradiation, etc. [28]. Thus, PS was selected in the present study as an alternative oxidant to improve the color and organic carbon removals from dyehouse effluent.

With the above-mentioned facts in mind, the present study aimed to explore the potential of a home-made LF photocatalyst to degrade an industrial model pollutant, namely the commercially important Reactive Black 5 (RB5) dye. The effect of the PS on the LF-mediated, photocatalytic treatment of synthetic dyehouse effluent was also examined using an aqueous, hydrolyzed (exhausted) RB5 solution. Moreover, the reuse potential of LF photocatalyst with LF/UV-A and PS/LF/UV-A treatments of RB5 and its dissolved organic carbon (here: DOC) content was also tested in the present study. The effect of PS on the photocatalytic of hydrolyzed RB5 solution was explained by carrying out additional baseline and control experiments, as well as following Fe and La release during photocatalytic and PS-enhanced photocatalytic treatment. Selected (most effective) treatment systems were applied to investigate their DOC removal performance in real water and wastewater samples, such as tap water (TW) and two secondary (biologically)-treated wastewaters (called WW-1, WW-2 herein).

2. Materials and methods

2.1. Materials

Home-made LF with a crystallite size of 43 nm and a Brunauer–Emmett–Teller surface area of 13 m^2/g was used in the photocatalytic experiments. The synthesis and characterization procedures were described in the previous work in detail [6]. The composition of the photocatalyst samples was confirmed via repeated scanning electron microscopy with energy-dispersive X-ray spectroscopy (SEM/EDX) analysis. RB5, selected as the commercially important, frequently studied model reactive dye was a gift from Eksoy Chemicals (Istanbul). For the photocatalytic experiments, a 0.4 g/L RB5 stock solution was prepared in hot (60°C–70°C) distilled water. 4.0 g/L of 12 N NaOH was added into the hot reaction solution to raise its pH above 11.0–11.5 and in this way to ensure complete hydrolysis of the dye [16]. During reactive dye hydrolysis, the reactive vinyl sulfone group of the dye is released that results in a bathochromic, red shift of the characteristic peaks of RB5 in the near-UV (300 ® 318 nm) as well as visible (597 ® 613 nm) light absorption bands [29]. The hydrolyzed RB5 stock solution was kept in the fridge (+4°C) during the experimental study. Hydrolyzed RB5 solution is very stable (resistant to chemical/photochemical/biochemical degradation) and thus can be safely used for several weeks if kept in a cool place. Prior to each run, the stock solution was adjusted to room temperature, diluted to 20 mg/L RB5 (the main working concentration in this study) with distilled water, then its pH was adjusted to the desired value. Aqueous, hydrolyzed RB5 solution was simply referred to as "RB5" herein. Tap water (TW) and two secondary treated sewage samples (WW-1, WW-2) were also treated in the later stages of this study. The two wastewater samples were taken from a local sewage treatment plant practicing secondary (biological activated sludge) treatment. The samples were stored in a fridge at +4°C prior to photocatalytic and enhanced photocatalytic experiments. The environmental characterization of TW and WW-1, WW-2

samples were presented in Tables S1 and S2, respectively. All other chemicals were purchased from Sigma-Aldrich Chemicals (USA). All reaction solutions were prepared with distilled water (<0.20 μS/cm). pH adjustment was done using HCl and NaOH solutions of different normalities (0.1–6 N).

2.2. Experimental procedures

All photocatalytic experiments were conducted in a three-neck quartz flask (h = 10 cm; r = 4 cm) where 500 mL of the prepared reaction solution was stirred at 100 rpm to supply oxygen near the saturation level (min. 8 mg/L as measured by means of an O_2 probe provided by WTW, Weilheim, Germany). The photochemical reaction chamber consisted of a LZC-ORG model (Luzchem Research Inc., Ontario, Canada) photoreactor (dimensions: 32 cm × 33 cm × 21 cm) equipped with a digitally controlled thermometer and a magnetic stirrer. The photochemical reaction chamber consisted of a maximum of ten fluorescent UV-A lamps (8 W each, emitting in the 300–400 nm wavelength region at λ_{max} = 365 nm) with a total incident light flux of I_o = 4,000 ± 100 lx (=1.3 W/L) which was controlled and calibrated by using the UV meter of the photoreactor. All of the ten UV-A lamps were turned on ca. 15 min prior to the experiment to obtain a stable UV-A light emission. In the LF/PS/UV-A experiments, PS was added at a molar ratio of 1:3 (0.6 mM PS) and 1:6 (1.2 mM PS) to the RB5 concentration (=0.2 mM; 20 mg/L) according to previous related work [4,7,11,30,31]. Samples were taken at regular time intervals and subjected to further analyses after centrifugation and/or other procedures if necessary. Photocatalysis and PS-enhanced (-assisted) photocatalysis were referred to as LF/UV-A and LF/PS/UVA in this work, respectively.

2.3. Analytical and instrumental procedures

Photocatalytically-treated samples were taken at regular time intervals from the photoreactor (t = 0–120, 180 and 210 min depending on the experimental concept) and centrifuged with a Hettich (Tuttlingen, Germany) model centrifuge at a speed of 5,000/6,000 rpm for 10 min. The color of the clear samples was measured at the peak absorbance value of hydrolyzed RB5 dye (λ_{max} = 610 nm) by a Jenway 6300 Model Spectrophotometer. A Shimadzu VPCN carbon analyzer (Japan) equipped with an autosampler was used for DOC analysis of the selected samples. A Thermo Orion 720A model pH-meter (Waltham, MA, USA) was used for pH measurements. La and Fe leaching was followed with an ICP Spectrometer (Perkin Elmer Optima 2100DV ICP-OES, Waltham, MA, USA). Lowest detection limits (LOD) were Fe = 0.05 mg/L and La = 0.1 mg/L. The environmental characterization of TW, WW-1 and WW-2 were carried out according to Standard Methods [32].

3. Results and discussion

3.1. Baseline and control experiments

Several baseline and control experiments (20 mg/L aqueous, hydrolyzed RB5; t = 120 min) were conducted to investigate the role of UV-A light, PS and pH on LF/UV-A and LF/PS/UV-A treatments. A pH of 7.5 was selected as the starting value for the experimental study since it is the typical pH of dyehouse effluent after pH re-adjustment [14,33,34] and mentioned as a suitable pH for LF-mediated photocatalytic treatment as well [4,35,36]. The control experiments consisted of the following changes in color (peak absorbance) values during RB5 treatment with 5 mM PS only, UV-A only and 0.6 mM PS/UV-A (in the absence of LF) at pH = 7.5 for 120 min. These experiments resulted in <5%, <5% and 41% color removals, respectively (Fig. S1). A PS/UV-A control experiment was also conducted at pH = 3.0 in order to obtain parallel data to the LF/UV-A and LF/PS/UV-A experiments carried out at acidic pH. These will be presented in the forthcoming sections. From Fig. S1 it is evident that for PS/UV-A treatment color removal increased from 41% to 83% when the pH was decreased from 7.5 to 3.0. It is known that UV-A irradiation can excite the electrons of the dye molecules from the highest occupied molecular orbital (HOMO) to the lowest unoccupied molecular orbital (LUMO) and these electrons may be accepted by PS to generate $SO_4^{\bullet -}$ and $HO^{\bullet}$ [28]. In this way, the dye molecule may act both as a photosensitizer and a substrate undergoing photodegradation. Moreover, the photoexcited dye is capable of oxidizing other substrate molecules through electron abstraction [35,37,38]. This speculatively could explain the substantial color removal being observed during PS/UV-A treatment of RB5 solution in the absence of LF.

3.2. Photocatalytic treatment of RB5 solution with LF/UV-A and LF/PS/UV-A processes

Several LF/UV-A experiments were run at varying photocatalyst concentrations (0.125–1.00 g/L) at neutral (=7.5) to alkaline (=10) pH with 10 and 20 mg/L RB5 solutions for t = 120 min. At this initial working stage, the reaction pH was kept in this range since it is a typical pH for the reactive dyeing process and dyebath effluent before and after pH adjustment with formic or acetic acid, respectively. For these experiments, color removal was always <10% (data not shown). Hence, it was decided to continue LF/UV-A and LF/PS/UV-A treatments of aqueous RB5 under acidic pH conditions to achieve photocatalytic color removal by dye degradation. It should also be mentioned here that considering previous work where preliminary dark adsorption + mixing was examined for LF, this period prior to photocatalytic treatment was fixed as around 5 min [6].

3.2.1. LF/UV-A experiments

The initial idea was to perform photocatalytic experiments either at the natural, alkaline pH of the RB5 solution (=10–12) or at neutral pH (=7.5), where the LF/UV-A process has proven to be most active in former related work [6,36,39]. However, no color removal due to either preliminary dark adsorption or photocatalytic degradation could be obtained for aqueous RB5 solution during these experiments in the 7.5–10.0 pH range (Fig. S2). As aforementioned, therefore it was decided to continue the LF-mediated photocatalytic experiments under acidic pH conditions and the reaction pH was adjusted to pH = 4 (LF/UV-A/pH4) and pH = 3 (LF/UV-A/pH3). From Figs. S2 and 1 it can be seen that when the reaction pH was adjusted to pH = 3, some minor but

still remarkable color removal (≤20%) occurred due to "preliminary dark adsorption" as a consequence of the electrostatic attraction between RB5 and LF. Preliminary dark RB5 adsorption rates were obtained as 13% and 20% at pH = 3 and pH = 4, respectively. Similar dark adsorption rates in the range of 22%–27% prior to photocatalysis have previously been reported for humic acid solutions treated with thermally modified LF, however at a neutral pH value [36]. The enhancement in photocatalytic color removal upon decreasing the initial pH of the reaction solution from pH = 4 to pH = 3 is demonstrated in Fig. 1.

As is apparent in Fig. 1, there is a huge difference in photocatalytic color removal profiles at pH = 4 and pH = 3. More specifically, the pH had to remain below 4 throughout the experiment to achieve efficient color removal. Color removal reached an asymptotic value of 20% for the experiment starting at an initial pH of 4 at t = 75 min, whereas 90% color removal was achieved after 90 min LF/UV-A treatment of aqueous RB5 at pH = 3 (Fig. 1). Hence, it may be concluded that RB5 degradation with the LF/UV-A process was strictly pH-dependent and not favorable at pH > 4. Undoubtedly, it is a surface phenomenon and also important for the DOC parameter. The degree of mineralization (ultimate oxidation) was also studied in this work. Fig. 2 depicts percent DOC removals obtained for LF/UV-A/pH3 treatment of 20 mg/L aqueous RB5 solutions at pH = 3. During LF/UV-A/pH4 treatment, no further DOC removal could be achieved than that removal due to dark adsorption onto LF (data not shown for LF/UV-A/pH4 treatment). According to Fig. 2, 17% of DOC removal already occurred during the preliminary dark adsorption stage (shown in Fig. 2 as percent DOC removal at t = 0 min).

Upon closer inspection of Fig. 2, it can be seen that in the initial stages of photocatalytic treatment where the

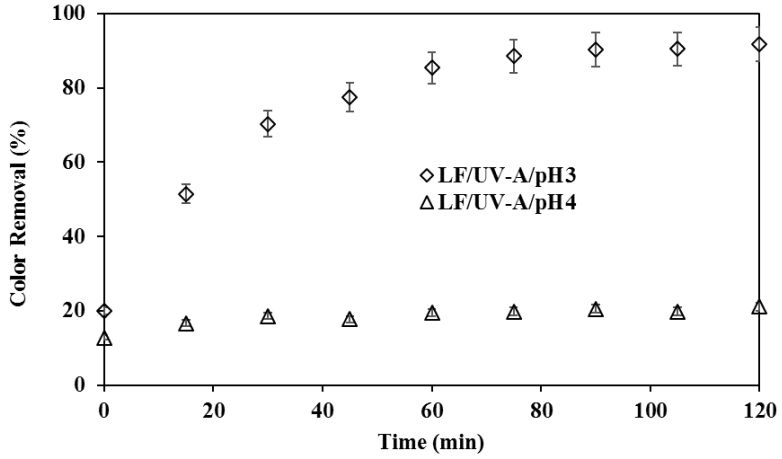

Fig. 1. Percent color removals obtained during LF/UV-A treatment of aqueous RB5 solution at pH = 3.0 and pH = 4.0. Conditions: RB5 = 20 mg/L; LF = 0.5 g/L; I_o = 1.3 W/L.

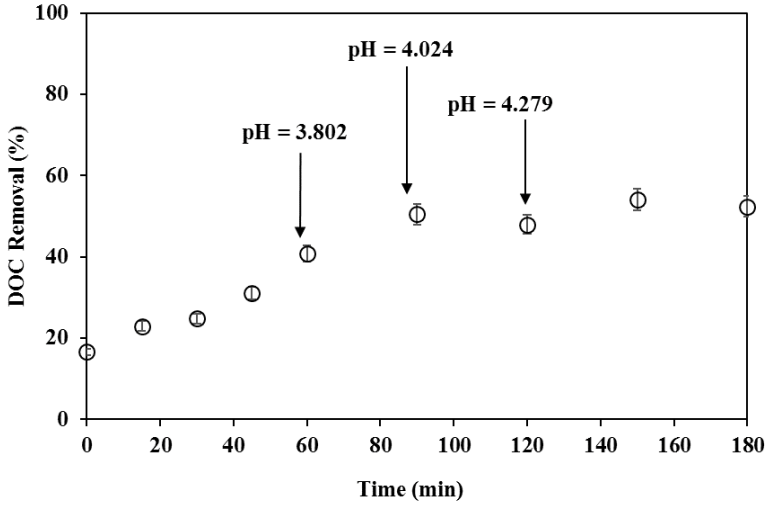

Fig. 2. Percent DOC removals obtained during LF/UV-A treatment of aqueous RB5 solution at pH = 3. The figure also indicates changes in pH values as evidence of the photocatalytic reaction slowing down with increasing pH. Conditions: RB5 = 20 mg/L; LF = 0.5 g/L; DOC_o = 5.15 mg/L; I_o = 1.3 W/L.

pH was still close to 3, DOC removal was rapid, although the pH of the reaction solution continued to increase. However, when the pH was above/close to 4, DOC removals abruptly slowed down reaching asymptotic values of 52%–54% at t = 90 min. the DOC removals only fluctuated between t = 90–180 min. So, it can be concluded that photocatalytic DOC removal followed a similar behavior to RB5 removal, and was pH-dependent. Moreover, the continuous rise in pH (some sample pH values that were inserted into Fig. 2) to pH > 4, negatively affected RB5 and DOC removal, which practically stopped after 90 min photocatalytic treatment. After 180 min treatment, the final pH of the reaction solution was pH = 4.6.

3.2.2. Effect of PS (LF/PS/UV-A/pH3 experiments)

Considering previous PS/UV treatment applications as well as studies about other PS-activation methods [29,30], it was expected that the addition of PS into the reaction solution would result in an enhancement both in terms of RB5 (color) and DOC (organic carbon) removals. In this part of the study, 0.6 and 1.2 mM PS were added to the LF/UV-A/pH3 treatment system to obtain a RB5:PS molar ratio of 1:3 and 1:6, respectively. PS concentrations, as well as the "target pollutant:PS" molar ratios, were selected considering previous related work where hydrogen peroxide was used as the peroxide for enhanced photocatalytic treatment [4,7,11,31]. Fig. 3 displays percent color removals (%) obtained during LF-mediated photocatalytic treatment in the presence of 0.6 and 1.2 mM PS.

From Fig. 3 it is evident that color removal with the LF/UV-A treatment system was appreciably enhanced in the presence of PS. Color removal was practically complete (>99%) in only 25–30 min and hence superior to PS/UV-A and LF/UV-A treatments at pH = 3. Upon closer inspection of Fig. 3, it is evident that the color removal profile of PS/UV-A/pH3, LF/PS/UV-A/pH3 and LF/UV-A/pH3 treatments follow different trends. The enhancement of LF/UV-A treatment in the presence of PS cannot be solely attributed to an additive effect of homogenous photochemical and heterogeneous photocatalytic reactions but rather synergistic effects of LF and PS coupled with UV-A irradiation. Considering previous work with LF/UV-A, it might be due to the interaction between the Fe ions released from and/or on the excited LF surface with PS (initiating photo-Fenton or Fenton-like reactions) or the direct interaction between the photo-generated conduction band electrons (e_{CB}^-) of the UV-A-excited LF surface and the oxidant PS, acting as an electron acceptor. In fact, color removal with the PS/UV-A/pH3 process proceeds slowly and steadily, ultimately reaching 83% after 120 min photochemical treatment. Some additional experiments and further measurements had to be conducted in order to elucidate the treatment mechanism that will be described later.

Fig. 4 presents overall percent DOC removals (%) obtained with LF/PS/UV-A/pH3 treatment (with 0.6 and 1.2 mM PS) compared with PS/UV-A/pH3 treatment for 120 min. DOC removals shown in Fig. 4 can also be compared with those shown in Fig. 2 for LF/UV-A treatment at acidic pH.

From Fig. 4 it is obvious that no DOC removal was obtained during RB5 treatment with PS/UV-A at pH = 3.0 (»3%; no DOC removal was obtained for PS/UV-A/pH7.5 – not shown data), indicating that PS/UV-A treatment is not capable of mineralization (ultimate oxidation) of RB5. Most probably, color removal during PS/UV-A treatment occurred with a different reaction mechanism and did not involve an indirect, free radical chain reaction. In fact, UV-A photolysis of PS is not expected to form $SO_4^{\bullet-}$ since UV-A does not provide sufficient photon energy for the homolytic photo-cleavage of PS. Fig. 4 also reveals that in the presence of LF, the oxidation of RB5 and its degradation products results in 60% and 66% DOC removal in the presence of 0.6 and 1.2 mM PS, respectively. However, in terms of color removal, there was no difference between using 0.6 and 1.2 mM PS during LF/PS/UV-A treatment (Fig. 3). Apparently, for ultimate oxidation (DOC removal), higher PS concentrations were needed so that not only RB5 but also its degradation products could

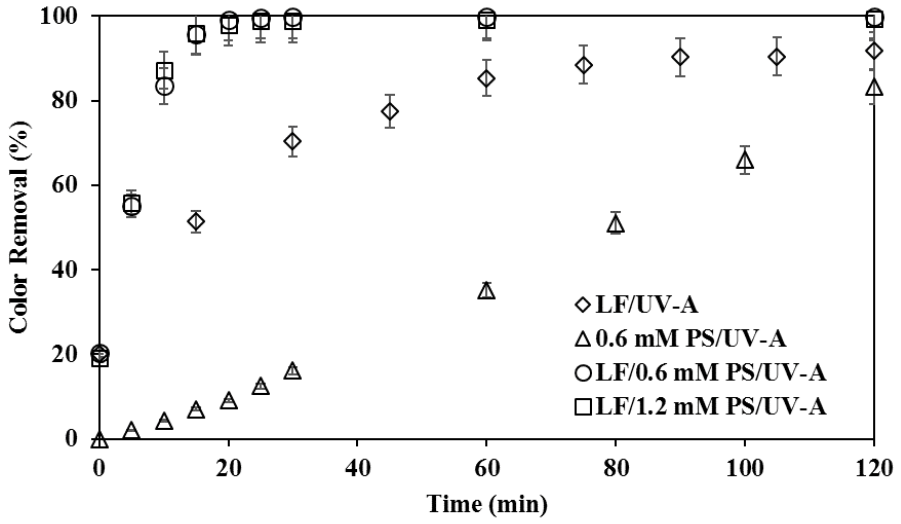

Fig. 3. Percent color removals obtained during different photocatalytic and photochemical treatments of aqueous RB5 solution at acidic pH values. Conditions: RB5 = 20 mg/L; LF = 0.5 g/L; pH = 3.0; I_o = 1.3 W/L.

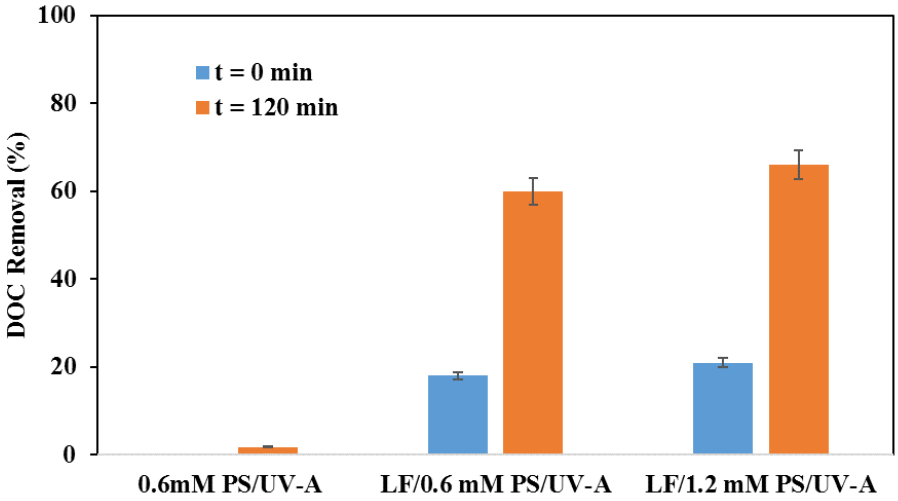

Fig. 4. Percent DOC removals obtained for the selected photocatalytic experiments with aqueous RB5 solutions. Conditions: RB5 = 20 mg/L; LF = 0.5 g/L; pH = 3.0; t = 120 min; DOC_o = 5.15 mg/L; I_o = 1.3 W/L.

be effectively oxidized. Among the tested treatment systems, the highest DOC removal was obtained for the LF/PS/UV-A process.

3.2.3. About the treatment mechanism of the LF/PS/UV-A process

A rather limited number of studies have investigated the reaction mechanism of perovskite-type oxides in the absence and presence of varying oxidants including peroxides [6,11,35,36,39,40]. Besides, no scientific work examined the role of PS in the LF/UV-A treatment of model pollutants. In order to explain the role of PS (the eventual enhancement due to PS addition) during LF-mediated treatment the following experimental sets were planned within the scope of this work;

- dark LF/pH3 (LF only) and dark LF/PS/pH3 experiments (in the absence of UV-A light)
- parallel measurement of La and Fe metals release during LF/UV-A/pH3 and LF/UV-A/PS/pH3 experiments

Experimental results of these two experimental sets are given in Fig. S3 (dark controls) and Fig. 5 (La and Fe metals release), respectively. According to Fig. S3, LF/pH3 and LF/PS/pH3 treatments in the absence of UV-A light lead to 47% and 56% color removals after 120 min, respectively. Since the color removal efficiencies and profiles look similar for these two control experiments, it can be concluded that a dark "Fenton-like reaction" that might be expected for LF/PS treatment of aqueous RB5 solution at pH3 can be ruled out since it did not have an additional contribution to color removal. Apparently, color removal was moderate (»50%) and occurred mainly due to preliminary (dark) RB5 adsorption onto the LF photocatalyst surface (Fig. S2). In fact, the RB5 dye is not only a high-molecular weight dye (991.8 g/mol) but also a large-molecule. Therefore, at least partly some hydrophobic interactions, as well as electrostatic attractions, are expected between RB5 and LF [6,19]. The LF surface (with a zero-point-of-charge of pH_{zpc} = 8.9 [41] is expected to possess a positive charge at pH = 3. It was principally expected that Fe on the LF surface interacts with the photogenerated e^-_{CB} and then the reduced form with PS in a heterogeneous "Fenton-like" redox reaction that could be involved in the PS activation and may result in the generation of $SO_4^{\bullet-}$ as proposed below in Eqs. (1) and (2):

$$\equiv Fe^{3+} + e^-_{CB} \rightarrow Fe^{2+} \quad (1)$$

$$\equiv Fe^{2+} + S_2O_8^{2-} \rightarrow Fe^{3+} + SO_4^{\bullet-} + SO_4^{2-} \quad k = 20\ M^{-1}\ s^{-1} \text{ at } 22°C \quad (2)$$

For instance, Luo et al. [4] reported that the degradation of the dye Rhodamine B was enhanced during treatment with $BiFeO_3$ nanoparticles in the presence of the peroxide H_2O_2 at a slightly acidic pH (=5) and proposed a reaction meachism for this heterogenelous catalytic redox reaction. However, in the present work RB5 color removals with LF and LF/PS at pH = 3 were rather close to each other (46% and 49% at t = 90 min; 47% and 56% at t = 120 min, respectively) and hence the "dark Fenton-like scenario" could not explain the superior RB5 removal for the LF/PS/UV-A/pH3 treatment system. In other words, considering the results of the dark control experiments most possibly there was another route involved in color removal from aqueous RB5 dye solution during heterogeneous photocatalytic treatment in the presence of PS. It is postulated that the direct interaction of the LF (Fe, La) surface with PS or more possibly the direct photocatalytic activation of PS with the photocatalytically produced conduction band electrons may become critical. The latter may take place as follows; the valence (VB) and conduction bands (CB) of perovskite are photo-excited by UV-A light-producing conduction band electrons (e^-_{CB}) and holes (h^+_{VB}) (Eq. (3) [28,43]) on the LF surface. The photo-generated e^-_{CB} react with PS to produce $SO_4^{\bullet-}$ (Eq. (4) [28]). Meanwhile, the h^+_{VB} reacts with H_2O forming $HO^{\bullet}$, simultaneously

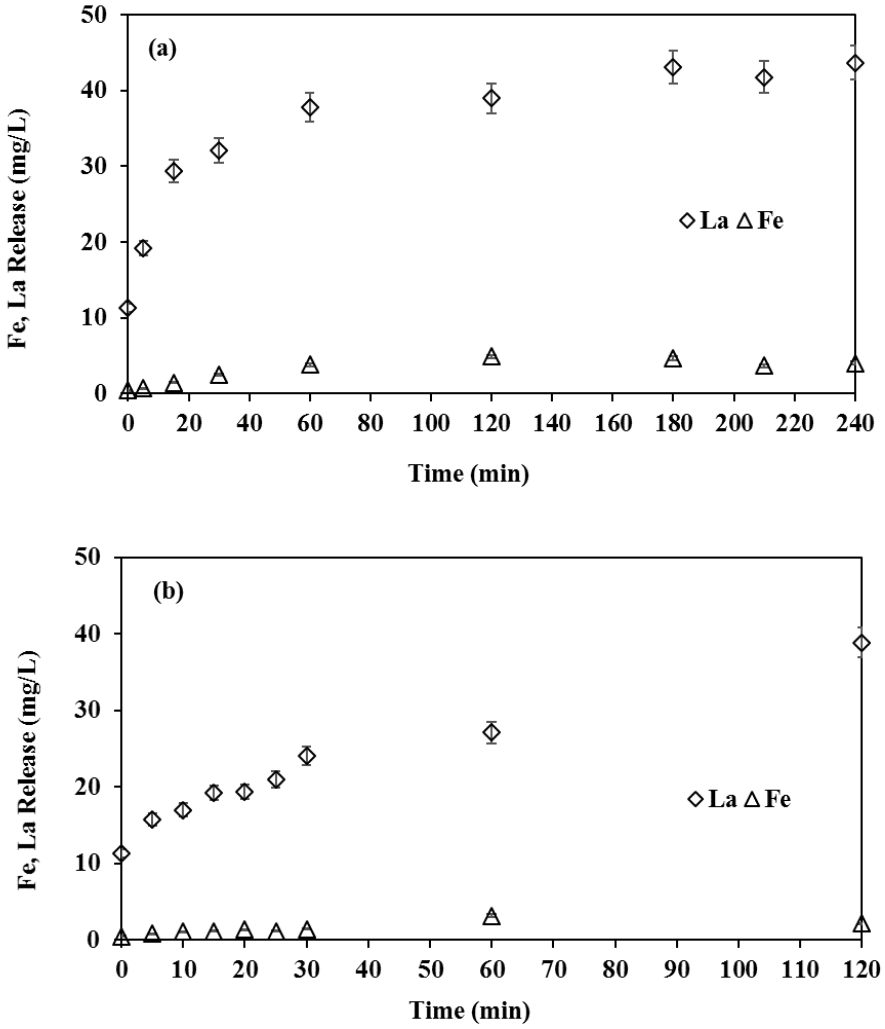

Fig. 5. Changes in Fe and La concentrations during LF/UV-A/pH3 (a) and LF/PS/UV-A/pH3 (b) treatments. Conditions: RB5 = 20 mg/L; LF = 0.5 g/L; PS = 0.6 mM; pH = 3.0; I_o = 1.3 W/L.

retarding the electron-hole recombination on LF (Eq. (5) [28]). The e^-_{CB} also react with O_2 producing $O_2^{\bullet-}$ radicals (Eq. (6) [28]). Hence, the redox reactions taking place between PS, H_2O, O_2 and Fe may increase the life time of h^+_{VB} and e^-_{CB} that drive the photocatalytic redox reactions. These collectively achieve the degradation of RB5 dye and its degradation products (Eq. (7) [28]) via free radical chain reactions ultimately leading to mineralization/ultimate oxidation end products (Eq. (8) [28]);

$$\text{Semiconductor}\left(\text{LF}\right)+\text{hv}\left(\lambda_{\max}=365\ \text{nm}\right)\rightarrow e^-_{CB}+h^+_{VB} \quad (3)$$

$$S_2O_8^{2-}+e^-_{CB}\rightarrow SO_4^{\bullet-}+SO_4^{2-} \quad (4)$$

$$h^+_{VB}+H_2O\rightarrow HO^{\bullet}+H^+ \quad (5)$$

$$e^-_{CB}+O_2\rightarrow O_2^{\bullet-} \quad (6)$$

$$h^+_{VB}/SO_4^{\bullet-}/HO^{\bullet}+\text{RB5}\left(\text{dye molecules}\right)\rightarrow \text{degradation products} \quad (7)$$

$$\text{RB5 / degradation products}\rightarrow\rightarrow CO_2+H_2O+NO_3^-+SO_4^{2-} \quad (8)$$

It is anticipated that in the present study both $HO^{\bullet}$ and $SO_4^{\bullet-}$ but mainly $SO_4^{\bullet-}$ might be actively involved in RB5 and its DOC removal. In order to elucidate the color removal mechanism during aqueous RB5 treatment, Fe and La releases were also followed during LF/UV-A and LF/PS/UV-A treatments under optimized, selected reaction conditions (20 mg/L hydrolyzed, aqueous RB5; 0.5 g/L LF; 0.6 mM PS; pH = 3.0; 1.3 W/L UV-A for 120 min LF/PS/UV-A and 240 min LF/UV-A treatment). The original (t = 0 min) La and Fe concentrations were 11.0 and 0.5 mg/L, respectively.

As evident from Fig. 5a, La and Fe values increased steadily during LF/UV-A treatment until 60 min. Beyond this treatment period, La and Fe started to reach asymptotic

values (they fluctuated) parallel to color removal which was also practically complete. On the other hand, La and Fe concentrations exhibited a different kinetic pattern during LF/PS/UV-A/pH3 treatment of aqueous RB5 solution as given in Fig. 5b. The increase in La concentrations was relatively slow and La remained practically constant between 5–25 min (at a concentration of 16–21 mg/L La). After 25–30 min LF/PS/UV-A treatment (time of complete color removal), La concentration increased more rapidly reaching 39 mg/L at t = 120 min. On the other hand, the Fe concentration remained constant between 10–30 min LF/PS/UV-A treatment at around 1.1–1.4 mg/L Fe in the reaction solution. Experimental results indicated that differences in La and Fe release profiles could be due to changes in the reaction mechanisms of LF/UV-A/pH3 and LF/PS/UV-A/pH3 treatment processes. It is speculatively thought that h^+_{VB} oxidation (parallel to Fe reduction by e^-_{CB}) of RB5 might play an important role in LF/UV-A treatment, whereas indirect oxidation of RB5 with $SO_4^{\bullet-}$ which is formed due to PS reduction by e^-_{CB} could also be critical for color removal with the LF/PS/UV-A process. The fact that the Fe concentration remains practically constant and La release is relatively slow during t = 5–25 min LF/PS/UV-A/pH3 treatment is interesting since during this time period the color of RB5 solution was completely removed with LF/PS/UV-A/pH3 treatment. This pattern indicated that during color removal rapid La and Fe release from the LF surface to the reaction bulk was hindered by the photocatalytic redox mechanism taking place on LF with Fe and La that were consumed/used due to reactions with h^+_{VB} and e^-_{CB}. In order to evaluate the stability of the catalyst and determine the role of a homogeneous Fenton-like reaction caused by leached Fe, an aqueous LF solution was stirred at pH = 4–5 for 24 h and analyzed for Fe after filtration [10]. Dissolved Fe was not detected in the filtered suspension thereby indicating that the homogeneous Fenton reaction mechanism was not involved in the degradation of the model pollutant under slightly acidic conditions [10]. Faye et al. [8] investigated Fe leaching from LF pH = 3 and pH = 4, similar to the pH conditions of the present work. Herein it was reported that released Fe was limited to a concentration of 2.7 mg/L even under acidic pH conditions for 0.5 g/L LF. However, acidic pH values might cause La and Fe leaching. In fact, in heterogeneous catalytic Fenton-like systems, pH can affect surface adsorption of the organic contaminant that is only relevant for charged compounds and changes in Fe speciation due to reduction of Fe(III) to Fe(II) by e^-_{CB} and/or $SO_4^{\bullet-}$. During the present work, the reaction pH never decreased to below 3.0, which is a pH known to negatively affect LF surface properties [8,44].

3.2.4. Reuse of the LF photocatalyst

Fe-containing catalysts usually suffer from leaching, particularly under acidic pH conditions. Perovskites on the other hand have an appreciably higher structural stability as confirmed by previous researchers [4,6,7,10,36,39]. The greater stability of LF over the traditional Fe-containing (photo) catalysts is an inherent advantage over other metal oxide catalysts. Poor regeneration of the oxidized metal in metal oxide catalysts back to its reduced state can take place in heterogeneous (photo)catalytic PS activation which ultimately results in the decay of catalytic activity. Fe and La leaching during photocatalytic treatment was already tested in previous work and no appreciable Fe or La leaching was observed for LF at neutral pH [7,10]. The stability and activity of different photocatalysts have already been demonstrated in previous work by conducting additional consecutive reuse experiments. In this work, LF was used in four (4) consecutive cycles during selected LF/UV-A/pH3 and LF/PS/UV-A/pH3 treatments of aqueous RB5. For that purpose, LF was centrifuged at 5000–6000 rpm for 5–10 min, rinsed twice with distilled water and dried at 105°C in an autoclave for 60 min. Then, another 20 mg/L aqueous RB5 solution was treated with the recovered LF under otherwise identical reaction conditions. This procedure was repeated in all consecutive treatment cycles 4 times in total (Figs. S4 and S5 for LF/UV-A and LF/PS/UV-A, respectively).

Fig. 6a depicts color and DOC removals during LF/UV-A/pH3 treatment of RB5. In terms of color removal, a slight decrease from 98% obtained in the 1st cycle to 90%, 91% and 92% in the next 3 treatment cycles was apparent. In terms of DOC removal, the decrease was more significant, namely from 62% to 15%, 11% and 11%, respectively, during the next three cycles of 210 min-photocatalytic treatment.

Since during the LF/UV-A/pH3 treatment process the interaction between RB5 as well as its degradation products with LF is critical, it is expected that upon continuous LF surface coverage with RB5 and its photocatalytic degradation products (collectively expressed here as the DOC parameter), the treatment performance of the 1st cycle will decrease. The performance reduction in terms of color and DOC parameters was most strongly observed in the 2nd cycle of the LF/UV-A treatment process, and a further reduction in color and DOC removal was only minor. From these results, it could be concluded that the multiple reuses of LF for color removal are feasible but not very suitable in terms of DOC removals that worsened appreciably due to the accumulation of dye intermediates onto the LF surface.

Fig. 6b displays percent color and DOC removals obtained during LF/PS/UV-A/pH3 treatment of aqueous RB5 solution (20 mg/L RB5; 0.5 g/L LF; 0.6 mM PS) for t = 120 min. From Fig. 6 it is evident that LF/PS/UV-A/pH3 treatment is superior in terms of color (always in the range of 99%–100%) as well as DOC (in the range of 59%–62%) removals in all treatment cycles. There was no reduction in treatment performance throughout the 4 treatment cycles involving LF/PS/UV-A/pH3 treatment due to the positive effect of PS addition on LF/UV-A treatment both in terms of color and DOC removal rates. The treatment performance of different perovskite oxide types during several reuse cycles was investigated in previous work [2,4,46]. Herein, it was reported that the investigated nanoparticles were quite stable and showed no loss of catalytic activity up to 5 treatment cycles. However, it should be mentioned that these studies were conducted at neutral pH values and the stability of the catalysts was solely based on the removal of target pollutants only in previous work [2,4,45,46]. To the best of our knowledge, there are no studies available on the treatment/reuse performance evaluation for a photocatalytic process in the presence of peroxides in terms of the DOC parameter which incorporates the organic carbon of the target pollutant as well as degradation intermediates and hence a major limitation of a catalyst material's reuse potential.

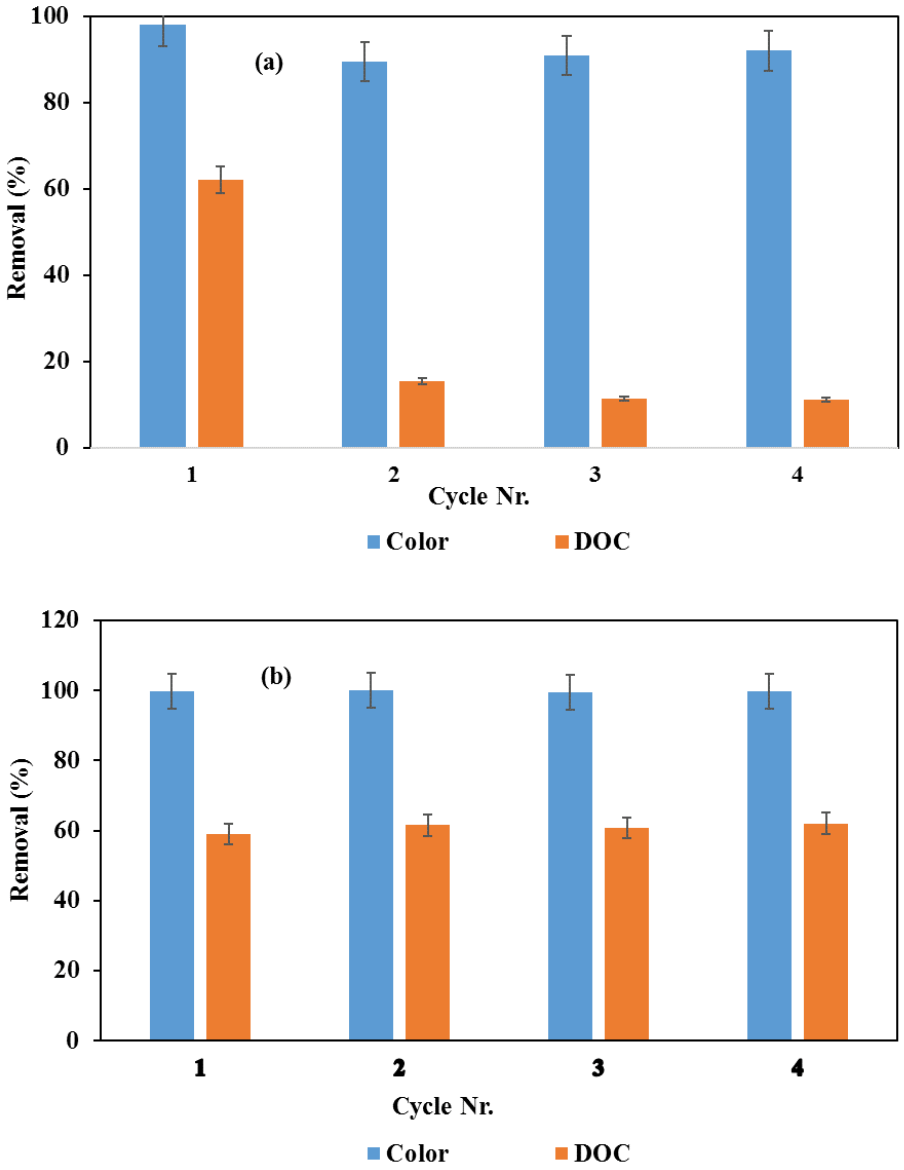

Fig. 6. Percent color and DOC removals obtained during LF/UV-A (a) and LF/PS/UV-A (b) treatments of RB5 in 4 consecutive cycles. Conditions: RB5 = 20 mg/L; LF = 0.5 g/L; pH = 3.0; DOC_o = 5.15 mg/L; $t_{(a)}$ = 210 min; $t_{(b)}$ = 120 min; I_o = 1.3 W/L.

3.3. Experiments with real tap water and secondary treated wastewater samples

In order to investigate the application potential of the selected photocatalytic treatment systems in real samples, experiments with tap water (TW) and two different biologically treated wastewater samples (WW-1, WW-2) were performed. LF/PS/UV-A/pH3 treatment with PS = 0.6 mM was proven to be the most favorable in terms of DOC removal in the treatability experiments conducted with WW-1 (data not shown). On the other hand, 1.2 mM PS was selected for LF/PS/UV-A/pH3 treatment of WW-2 since this wastewater sample exhibited a higher organic carbon content (Table S2) and thus eventually required a higher PS concentration. The environmental characterization of TW and WW-1, WW-2 samples were presented in Tables S1 and S2, respectively. Fig. 7 shows the percent DOC removals obtained for the LF/PS/UV-A/pH3 treatment of the TW, WW-1 and WW-2 samples.

As is obvious in Fig. 7, DOC removals decreased for the real water and wastewater samples compared with those observed for aqueous RB5 solution, although the DOC value for TW and WW-2 did not differ appreciably from the DOC content of 20 mg/L RB5 solution. The DOC removal due to "preliminary dark adsorption" also decreased from 18%–21% for the aqueous RB5 solution (Fig. 4) to 8.2%, 1.8% and 4.4% for TW, WW-1, and WW-2, respectively. At the end of the photocatalytic treatment, overall DOC removals were obtained as 25% and 22% for TW and WW-1, respectively. Despite the higher concentration of PS used in the photocatalytic treatment of WW-2 that exhibited a stronger (higher) DOC content, a relatively low DOC removal of only

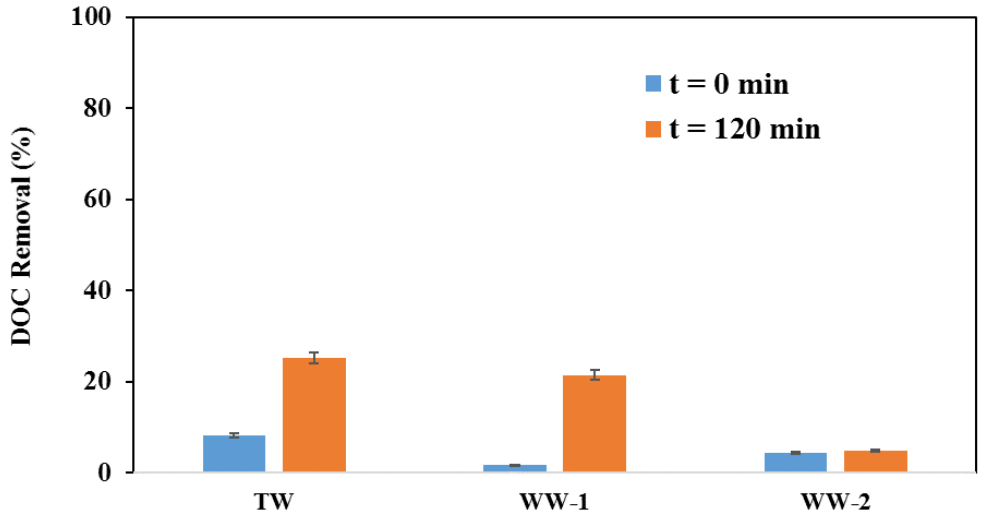

Fig. 7. Percent DOC removals obtained for LF/PS/UV-A treatment of TW, WW-1 and WW-2. Time t = 0 indicates percent DOC removal due to preliminary dark adsorption onto the LF photocatalyst. Conditions: RB5 = 20 mg/L; LF = 0.5 g/L; pH = 3.0; t = 120 min; $DOC_{o,TW}$ = 1.98 ± 0.11 mg/L, $DOC_{o,WW\text{-}1}$ = 5.39 mg/L, $DOC_{o,WW\text{-}2}$ = 16.83 mg/L; I_o = 1.3 W/L.

5% could be achieved for this wastewater sample. From the above results, it may be concluded that the DOC removals were significantly inhibited due to the presence of various organic and inorganic compounds and particularly the higher organic carbon content in the biotreated sewage sample. The effect of different organic and inorganic ions present in real water/wastewater matrices on the photocatalytic/photochemical treatment performance was already investigated in some recent work [46–48]. A negative (inhibitory) effect was typically observed in terms of target pollutant removal performance at elevated concentrations of humic acid, chloride, phosphate, or sulfate, depending on the concentration (inorganics >250–500 mg/L; humic acid >10–20 mg/L) and type of added ions [48,49]. Only limited information is available on the application of perovskite-type materials for the treatment of real water/wastewater samples. Jing et al. [48] reported that total organic carbon (TOC) removals decreased dramatically in Bisphenol A-containing food wastewater similar to the results of the present work. Apparently, not only the concentration but also the type/nature of the organic/inorganic substrates in the water/wastewater sample may affect the treatment performance of the target pollutant. It should also be pointed out here that the concentration of peroxides (here: PS) has a pivotal role in $SO_4^{\bullet-}$-based AOPs. Although higher concentrations of PS might be requied fort he treatment of real water and wastewater it has also been reported that excessive concentrations of peroxides (here: PS) might scavenge $HO^{\bullet}$ to for persulfate radicals ($S_2O_8^{\bullet-}$) as shown below [50,51];

$$S_2O_8^{2-} + HO^{\bullet} \rightarrow S_2O_8^{\bullet-} + HO^{-} \quad (9)$$

As aforementioned, $S_2O_8^{\bullet-}$ are less powerful and hence more selective/long-lived than $SO_4^{\bullet-}$. This could have positive as well as negative effects on $SO_4^{\bullet-}$-based advanced oxidation of real industrial wastewater depending on the wastewater constituents.

4. Conclusions

A home-made lanthanum iron oxide (LF) was used for the photocatalytic and persulfate (PS)-enhanced photocatalytic treatment of an industrial model pollutant in synthetic wastewater as well as real water and wastewater samples. The experimental study focused on the effect of pH and PS addition to explain the treatment mechanism of enhanced LF-mediated photocatalysis. pH played a critical role in LF-mediated heterogeneous photocatalysis of the model industrial pollutant (hydrolyzed, aqueous RB5 solution) and the pH had to be kept ≤ 4 to achieve substantial color and organic carbon (DOC) removals. Moreover, PS addition had a profound effect on color and organic carbon removals. The positive effect of PS was attributable to its role as an electron scavenger and its reaction with photocatalytically reduced Fe in the LF lattice forming sulfate radicals. These, in turn, would react with RB5 and its degradation products. The addition of the PS also improved the reuse performance of LF; multiple use was possible accompanied by complete color and highly efficient DOC removals. PS-enhanced photocatalytic treatment was also applied to treat real water (tap water and secondary/biologically treated wastewater). DOC removal was still observed during PS-enhanced photocatalytic treatment; however, treatment (DOC removal) performance decreased appreciably due to the complexity and higher DOC content of the real water/wastewater samples. However, it should be emphasized there that the peroxide (here: PS) concentration and reaction time were kept relatively low compared to previous work dealing with LF/UV-A treatments. In real-scale applications where complex effluents such as textile industry wastewater/dyehouse effluent has to be treated, the potential of using for instance natural, solar light as the UV-A light source for LF/PS/UV-A treatment could be explored to save operating costs associated with the electricity required to run the UV-A lamps. Further, adjusting/optimizing the heterogeneous photocatalytic process to "real" (more complex and harsher) conditions would improve the treatment results.

The possibility to use the LF photocatalyst multiple times is a very exciting and promising feature of the proposed treatment system. In this way, PS-enhanced, LF-mediated photocatalysis could be considered as an alternative, promising treatment method for refractory industrial pollutants found in water and wastewater including reactive dyes.

Disclosure statement

The authors have no competing interests to declare.

Funding details

This work was supported by the Istanbul Technical University under Project MAB-2021–43188. The authors are thankful to Eksoy Chemicals for the gift reactive dye sample.

References

[1] M.A. Peña, J.L.G. Fierro, Chemical structures and performance of perovskite oxides, Chem. Rev., 101 (2001) 1981–2017.
[2] F. Parrino, E. García-López, G. Marcì, L. Palmisano, V. Felice, I.N. Sora, L. Armelao, Cu-substituted lanthanum ferrite perovskites: preparation, characterization and photocatalytic activity in gas-solid regime under simulated solar light irradiation, J. Alloys Compd., 682 (2016) 686–694.
[3] F. Zurlo, E. Di Bartolomeo, A. D'Epifanio, V. Felice, I.N. Sora, L. Tortora, S. Licoccia, $La_{0.8}Sr_{0.2}Fe_{0.8}Cu_{0.2}O_{3-\delta}$ as "cobalt-free" cathode for $La_{0.8}Sr_{0.2}Ga_{0.8}Mg_{0.2}O_{3-\delta}$ electrolyte, J. Power Sources, 271 (2014) 187–194.
[4] W. Luo, L.H. Zhu, N. Wang, H.Q. Tang, M.J. Cao, Y.B. She, Efficient removal of organic pollutants with magnetic nanoscaled $BiFeO_3$ as a reusable heterogeneous Fenton-like catalyst, Environ. Sci. Technol., 44 (2010) 1786–1791.
[5] X. Chen, W. Wang, H. Xiao, C. Hong, F. Zhu, Y. Yao, Z. Xue, Accelerated TiO_2 photocatalytic degradation of Acid Orange 7 under visible light mediated by peroxymonosulfate, Chem. Eng. J., 193–194 (2012) 290–295.
[6] N. Türkten, I.N. Sora, A. Tomruk, M. Bekbölet, Photocatalytic degradation of humic acids using $LaFeO_3$, Catalysts, 8 (2018), doi: 10.3390/catal8120630.
[7] K. Wang, H. Niua, J. Chen, J. Song, C. Mao, M. Zhang, Y. Gao, Immobilizing $LaFeO_3$ nanoparticles on carbon spheres for enhanced heterogeneous photo-Fenton like performance, Appl. Surf. Sci., 404 (2017) 138–145.
[8] J. Faye, E. Guelou, J. Barrault, J.M. Tatibouet, S. Valange, $LaFeO_3$ perovskite as new and performant catalyst for the wet peroxide oxidation of organic pollutants in ambient conditions, Top Catal., 52 (2009) 1211–1219.
[9] H.Y. Zhao, J.L. Cao, H.L. Lv, Y.B. Wang, G.H. Zhao, 3D nanoscale perovskite-based composite as Fenton-like system for efficient oxidative degradation of ketoprofen, Catal. Commun., 41 (2013) 87–90.
[10] K. Rusevova, R. Köferstein, M. Rosell, H.H. Richnow, F.-D. Kopinke, A. Georgi, $LaFeO_3$ and $BiFeO_3$ perovskites as nanocatalysts for contaminant degradation in heterogeneous Fenton-like reactions, Chem. Eng. J., 239 (2014) 322–331.
[11] N. Sora, D. Fumagalli, Fast photocatalytic degradation of pharmaceutical micropollutants and ecotoxicological effects, Environ. Sci. Pollut. Res., 24 (2017) 12556–12561.
[12] M.H. Kim, C.H. Hwang; S. Bin Kang, S. Kim, S.W. Park, Y.S. Yun, S.W. Won, Removal of hydrolyzed Reactive Black 5 from aqueous solution using a polyethylenimine-polyvinyl chloride composite fiber, Chem. Eng. J., 280 (2015) 18–25.
[13] C.H. Neoh, C.Y. Lam, C.K. Lim, A. Yahya, H.H. Bay, Z. Ibrahim, Z.Z. Noor, Biodecolorization of recalcitrant dye as the sole source of nutrition using *Curvularia clavata* NZ_2 and decolorization ability of its crude enzymes, Environ. Sci. Pollut. Res., 22 (2015) 11669–11678.
[14] L. Bilińska, M. Gmurek, S. Ledakowicz, Comparison between industrial and simulated textile wastewater treatment by AOPs-biodegradability, toxicity and cost assessment, Chem. Eng. J., 306 (2016) 550–559.
[15] A. Reife, H.S. Freeman, Environmental Chemistry of Dyes and Pigments, Wiley, New York, 1996, p. 329.
[16] H.S. Freeman, A. Reife, Dyes, Environmental Chemistry, Kirk-Othmer, Ed., Encyclopedia of Chemical Technology, 4th ed., John Wiley & Sons, Inc., Hoboken, New Jersey, 2003, pp. 431–463.
[17] M. Bilal, T. Rasheed, H.M.N. Iqbal, H. Hu, W. Wang, X. Zhang, Toxicological assessment and UV/TiO_2-based induced degradation profile of Reactive Black 5 dye, J. Environ. Manage., 61 (2018) 171–180.
[18] I. Grčić, S. Papić, D. Mesec, N. Koprivanac, D. Vujević, The kinetics and efficiency of UV assisted advanced oxidation of various types of commercial organic dyes in water, J. Photochem. Photobiol., A, 273 (2014) 49–58.
[19] H. Saroyan, D. Ntagiou, K. Rekos, E. Deliyanni, Reactive Black 5 degradation on manganese oxides supported on sodium hydroxide modified graphene oxide, Appl. Sci., 9 (2019) 2167, doi: 10.3390/app9102167.
[20] The Central Pollution Control Board (CPCB), Environmental Standards for Ambient Air, Automobiles, Fuels, Industries and Noise, CPCB-New Delhi, 2000, p. 119.
[21] United States Environmental Protection Agency (US EPA), Office of Wastewater Management, National Risk Management Research Laboratory, US Agency for International Development, Guideline-Water-Reuse, Washington, DC, 2012, p. 643.
[22] A.K. Pikaev, V.I. Zolotarevskii, Pulse radiolysis of aqueous solutions of sulfuric acid, Bull. Acad. Sci. USSR, Div. Chem. Sci., 16 (1967) 181–182.
[23] P. Neta, R.E. Huie, A.B. Ross, Rate constants for reactions of inorganic radicals in aqueous solution, J. Phys. Chem. Ref. Data, 17 (1988) 1027–1284.
[24] G.V. Buxton, C.L. Greenstock, W.P. Helman, A.B. Ross, Critical review of rate constants for reactions of hydrated electrons, hydrogen atoms and hydroxyl radicals ($^{\bullet}OH/^{\bullet}O^{-}$) in aqueous solution, J. Phys. Chem. Ref. Data, 17 (1988) 513–886.
[25] M. Yousefi, F. Ghanbari, M.A. Zazouli, S. Madihi-Bidgoli, Brilliant Blue FCF degradation by persulfate/zero valent iron: the effects of influencing parameters and anions, Desal. Water Treat., 70 (2017) 364–371.
[26] X. Ding, L. Gutierrez, J.P. Croue, M. Li, L. Wang, Y. Wang, Hydroxyl and sulfate radical-based oxidation of RhB dye in UV/H_2O_2 and UV/persulfate systems: kinetics, mechanisms, and comparison, Chemosphere, 253 (2020) 126655, doi: 10.1016/j.chemosphere.2020.126655.
[27] M. Dogan, T. Öztürk, T. Ölmez-Hanci, I. Arslan-Alaton, Persulfate and hydrogen peroxide-activated degradation of Bisphenol A with nano-scale zero-valent iron and aluminum, J. Adv. Oxid. Technol., 19 (2016) 266–275.
[28] J. Yang, M. Zhu, D.D. Dionysiou, What is the role of light in persulfate-based advanced oxidation for water treatment?, Water Res., 189 (2021) 116627, doi: 10.1016/j.watres.2020.116627.
[29] J. Shore, Cellulosics Dyeing, The Society of Dyers and Colorists, Alden Press, Oxford, 1995, p. 408.
[30] I. Arslan-Alaton, A. Karatas, Ö. Pehlivan, O. Koba-Ucun, T. Ölmez-Hanci, Effect of UV-A-assisted iron-based and UV-C-driven oxidation processes on organic matter and antibiotic resistance removal in tertiary treated urban wastewater, Catal. Today, 361 (2020) 152–158.
[31] Q. Yang, Y. Ma, F. Chen, F. Yao, J. Sun, S. Wang, K. Yi, L. Hou, X. Li, D. Wang, Recent advances in photo-activated sulfate radical-advanced oxidation process (SR-AOP) for refractory organic pollutants removal in water, Chem. Eng. J., 378 (2019) 122149, doi: 10.1016/j.cej.2019.122149.
[32] APHA-AWWA-WEF, Standard Methods for the Examination of Water and Wastewater, R.B. Rice, A.D. Baird, Eds., 22nd ed., American Public Health Association (APHA), American Water Works Association (AWWA), Water Environment Federation (WEF), Washington, D.C., 2012, p. 1496.

[33] I. Arslan Alaton, I. Akmehmet Balcioglu, Photochemical and heterogeneous photocatalytic degradation of waste vinylsulphone dyes: a case study with hydrolyzed Reactive Black 5, J. Photochem. Photobiol., A, 141 (2001) 247–254.
[34] N.H. Ince, G. Tezcanli, Reactive dyestuff degradation by combined sonolysis and ozonation, Dyes Pigm., 49 (2001) 145–153.
[35] S. Li, L. Jing, W. Fu, L. Yang, B. Xin, H. Fu, Photoinduced charge property of nanosized perovskite-type $LaFeO_3$ and its relationships with photocatalytic activity under visible irradiation, Mater. Res. Bull., 42 (2007) 203–212.
[36] N. Yahya, F. Aziz, J. Jaafar, W.J. Lau, N. Yusof, W.N.W. Salleh, A.F. Ismail, M. Aziz, Impacts of annealing temperature on morphological, optical and photocatalytic properties of gel-combustion-derived $LaFeO_3$ nanoparticles, Arabian J. Sci. Eng., 46 (2021) 6153–6165.
[37] J.L. Wang, L.J. Xu, Advanced oxidation processes for wastewater treatment: formation of hydroxyl radical and application, Crit. Rev. Env. Sci. Technol., 42 (2012) 251–325.
[38] I. Khan, K. Saeed, I. Zekker, B. Zhang, A.H. Hendi, A. Ahmad, S. Ahmad, N. Zada, H. Ahmad, L.A. Shah, T. Shah, I. Khan, Review on Methylene blue: its properties, uses, toxicity and photodegradation, Water, 14 (2022) 242, doi: 10.3390/w14020242.
[39] S. Thirumalairajan, K. Girija, I. Ganesh, D. Mangalaraj, C. Viswanathan, A. Balamurugan, N. Ponpandian, Controlled synthesis of perovskite $LaFeO_3$ microsphere composed of nanoparticles via self-assembly process and their associated photocatalytic activity, Chem. Eng. J., 209 (2012) 420–428.
[40] L. Ju, Z. Chen, L. Fang, W. Dong, F. Zheng, M. Shen, Sol-gel synthesis and photo-Fenton-like catalytic activity of $EuFeO_3$ nanoparticles, J. Am. Ceram. Soc., 94 (2011) 3418–3424.
[41] N.C. Birben, E. Lale, R. Pelosato, N. Türkten, I.N. Sora, M. Bekbölet, Photocatalytic bactericidal performance of $LaFeO_3$ under solar light in the presence of natural organic matter: spectroscopic and mechanistic evaluation, Water, 13 (2021), doi: 10.3390/w13192785.
[42] S.Y. Oh, S.G. Kang, P.C. Chiu, Degradation of 2,4-dinitrotoluene by persulfate activated with zero-valent iron, Sci. Total Environ., 408 (2010) 3464–3468.
[43] S. Zhang, S. Song, P. Gu, R. Ma, D. Wei, G. Zhao, T. Wen, R. Jehan, B. Hu, X. Wang, Visible-light-driven activation of persulfate over cyano and hydroxyl group co-modified mesoporous g-C_3N_4 for boosting bisphenol A degradation, J. Mater. Chem. A, 7 (2019) 5552–5560.
[44] K. Rusevova, F.D. Kopinke, A. Georgi, Nano-sized magnetic iron oxides as catalysts for heterogeneous Fenton-like reactions-influence of Fe(II)/Fe(III) ratio on catalytic performance, J. Hazard. Mater., 241–242 (2012) 433–440.
[45] A. Kumar, M. Chandel, M.A. Sharma, M. Thakur, A. Kumar, D. Pathania, L. Singh, Robust visible light active PANI/$LaFeO_3$/$CoFe_2O_4$ ternary heterojunction for the photo-degradation and mineralization of pharmaceutical effluent: clozapine, J. Environ. Chem. Eng., 9 (2021) 106159, doi: 10.1016/j.jece.2021.106159.
[46] J. Jing, C. Cao, S. Ma, Z. Li, G. Qu, B. Xie, W. Jin, Y. Zhao, Enhanced defect oxygen of $LaFeO_3$/GO hybrids in promoting persulfate activation for selective and efficient elimination of bisphenol A in food wastewater, Chem. Eng. J., 407 (2021) 126890, doi: 10.1016/j.cej.2020.126890.
[47] I. Arslan-Alaton, T. Ölmez-Hanci, T. Öztürk, Effect of inorganic and organic solutes on zero-valent aluminum-activated hydrogen peroxide and persulfate oxidation of bisphenol A, Environ. Sci. Pollut. Res., 25 (2018) 34938–34949.
[48] Ö. Tuna, S. Karadirek, E.B. Simsek, Deposition of $CaFe_2O_4$ and $LaFeO_3$ perovskites on polyurethane filter: a new photocatalytic support for flowthrough degradation of tetracycline antibiotic, Environ. Res., 2022 (2005) 112389, doi: 10.1016/j.envres.2021.112389.
[49] R. Pelosato, V. Carrara, I.N. Sora, Enhanced photocatalytic degradation of ibuprofen in aqueous solution under visible-light irradiation: effects of $LaFeO_3$ and Cu/$LaFeO_3$, Chem. Eng. Trans., 73 (2019) 181–186.
[50] T. Ölmez-Hanci, I. Arslan-Alaton, Comparison of sulfate and hydroxyl radical based advanced oxidation of phenol, Chem. Eng. J., 224 (2013) 10–16.
[51] S. Giannakis, K.-Y. Andrew Lin, F. Ghanbari, A review of the recent advances on the treatment of industrial wastewaters by sulfate radical-based advanced oxidation processes (SR-AOPs), Chem. Eng. J., 406 (2021) 127083, doi: 10.1016/j.cej.2020.127083.

Supplementary information

Table S1
Environmental characteristics of the tap water (TW) sample

Parameter	Value
TOC (mg/L)	2.83
DOC (mg/L)	1.98
Alkalinity (mg $CaCO_3$/L)	100
Color (Pt-Co)	10
Conductivity (μS/cm)	435
Cl^- (mg/L)	42.5
SO_4^{2-} (mg/L)	38.2
NO_3^- (mg/L)	4.7
pH	8.0

Table S2
Environmental characteristics of the biologically (secondary) treated wastewater (sewage) samples (WW-1, WW-2)

Parameter (units)	WW-1	WW-2
TOC (mg/L)	18.68	24.43
DOC (mg/L)	5.39	16.83
COD (mg/L)	<30	<30
TSS (mg/L)	52.5	162.5
VSS (mg/L)	37.5	110
Color (Pt-Co)	11	60
Alkalinity (mg $CaCO_3$/L)	96	314
Conductivity (μS/cm)	2,390	7,800
SO_4^{2-} (mg/L)	87	288
NO_3^- (mg/L)	7.38	13.41
PO_4^{3-} (mg/L)	3.67	13.34
Cl^- (mg/L)	571	2,005
Br^- (mg/L)	1.81	10.63
pH	7.23	7.02

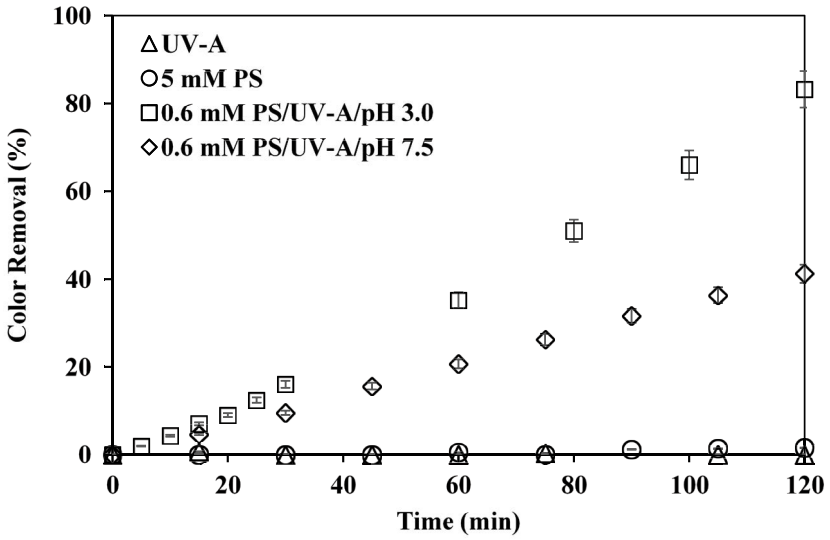

Fig. S1. Percent color removals obtained during some control experiments. Conditions: RB5 = 20 mg/L; I_o = 1.3 W/L.

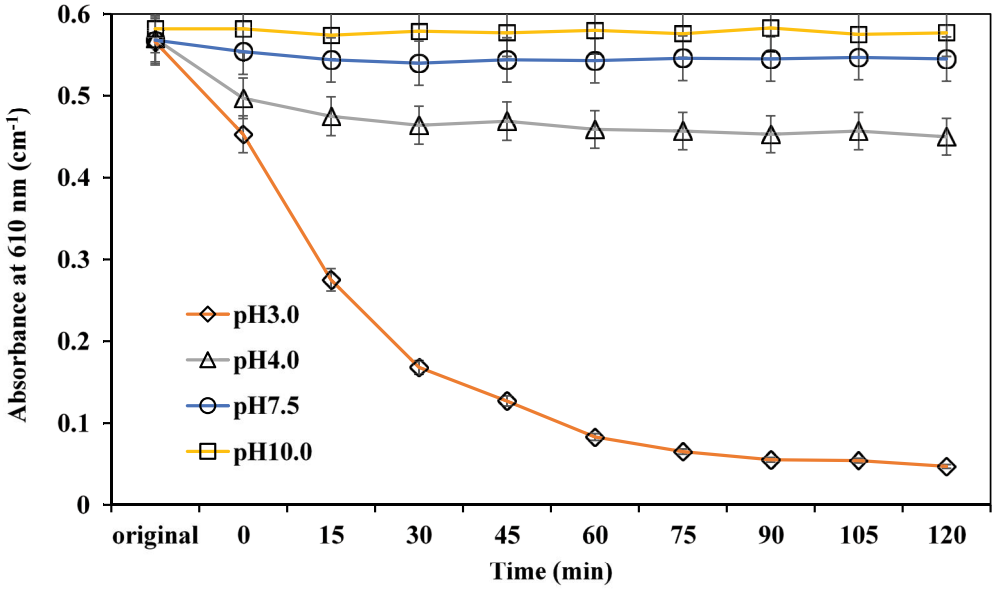

Fig. S2. Changes in (peak) absorbance at 610 nm values during LF/UV-A experiments conducted at varying pH values. The "dark" mixing and preliminary adsorption time were fixed at 5 min ("original" value). Conditions: RB5 = 20 mg/L; LF = 0.5 g/L; A_o = 0.577 cm^{-1} at 610 nm; I_o = 1.3 W/L.

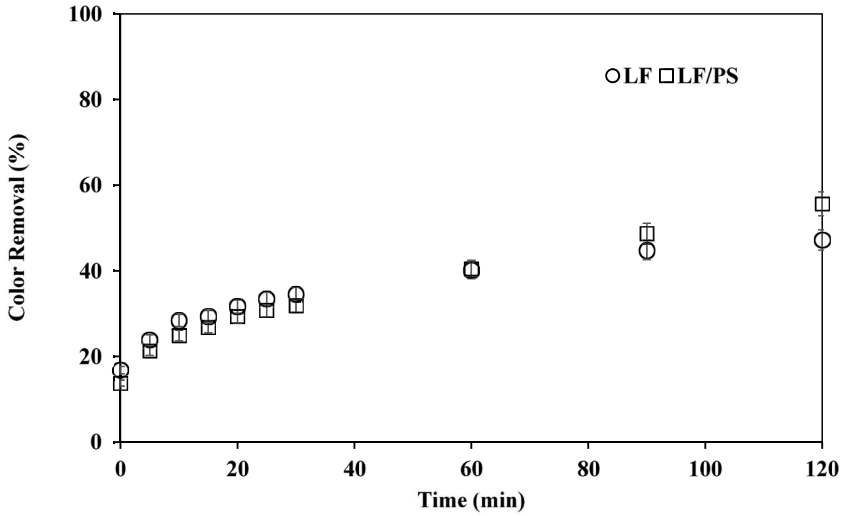

Fig. S3. Percent color removals obtained during the "dark" control (baseline) experiments with LF and LF/PS. Conditions: RB5 = 20 mg/L; LF = 0.5 g/L; PS = 0.6 mM; pH = 3.0.

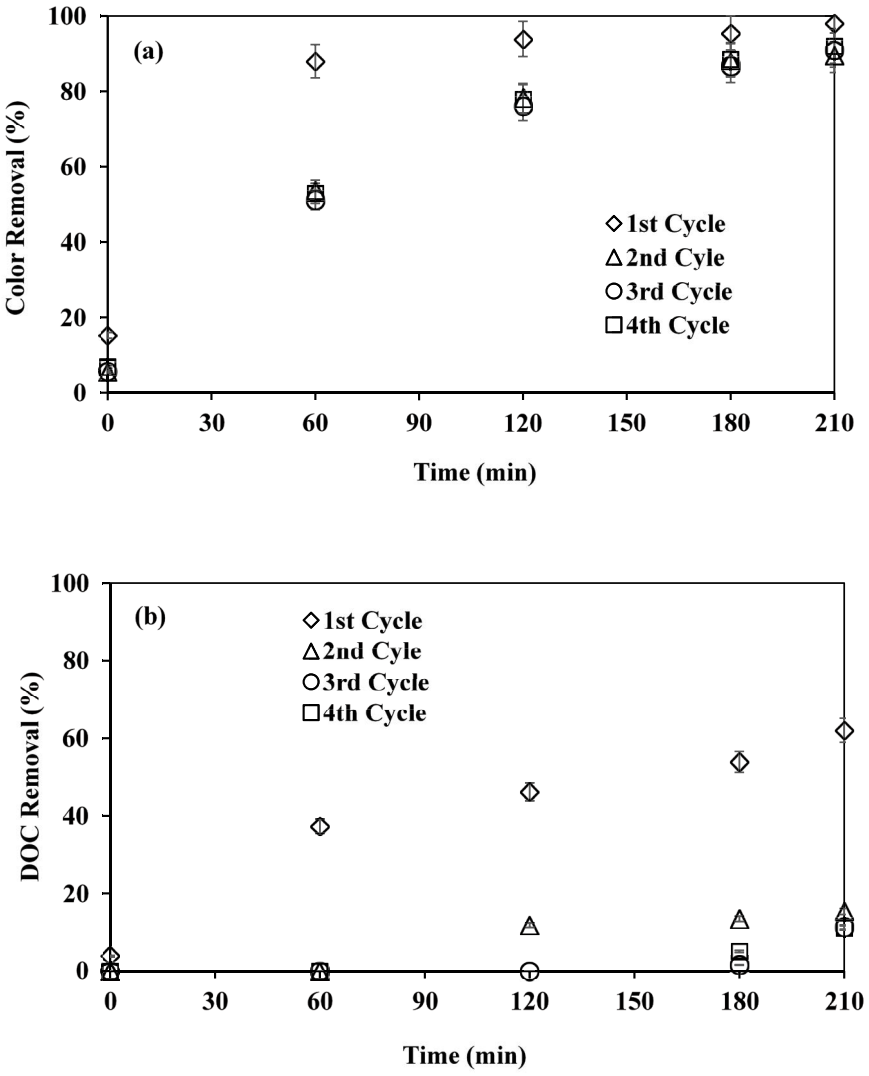

Fig. S4. Percent color (a) and DOC (b) removals obtained during LF/UV-A treatment of RB5 in four (4) consecutive cycles. Conditions: RB5 = 20 mg/L; LF = 0.5 g/L; pH = 3.0; DOC_o = 5.15 mg/L; I_o = 1.3 W/L.

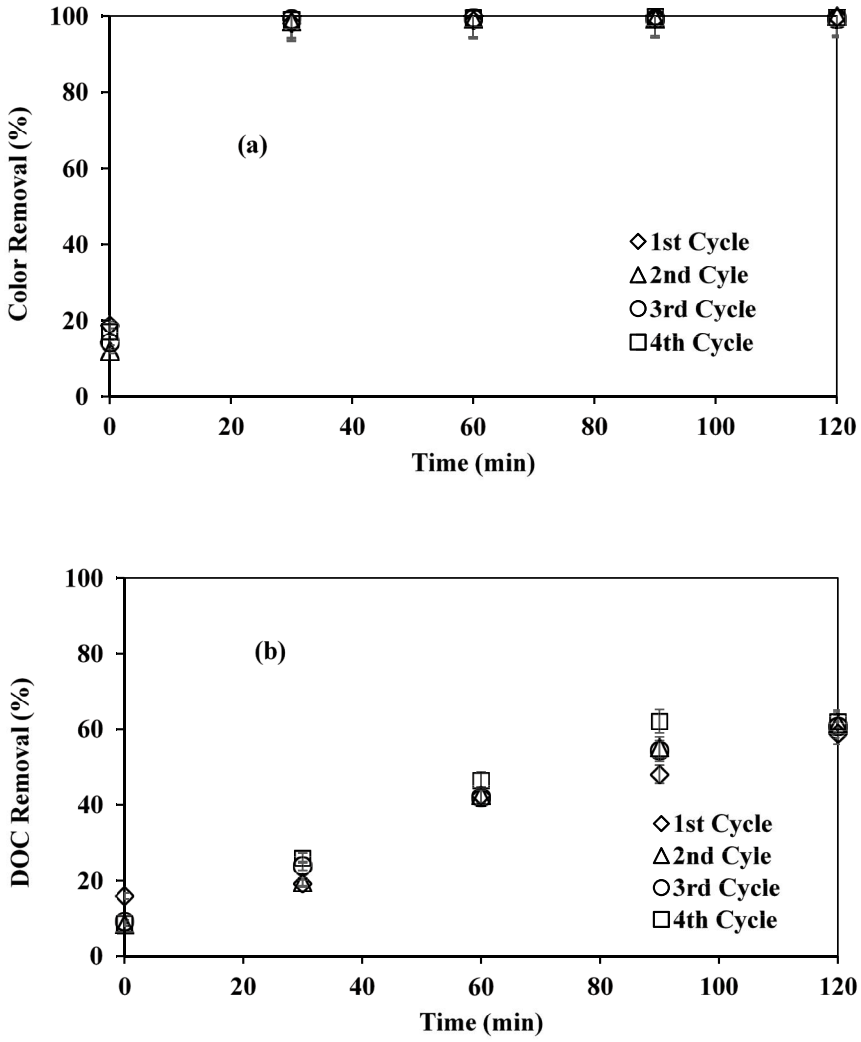

Fig. S5. Percent color (a) and DOC (b) removals obtained during LF/PS/UV-A treatment of RB5 in four (4) consecutive cycles. Conditions: RB5 = 20 mg/L; LF = 0.5 g/L; PS = 0.6 mM; pH = 3.0; DOC_o = 5.15 mg/L; I_o = 1.3 W/L.